IIETA International Information and Engineering Technology Association
Advancing the World of Information and Engineering

Annales de Chimie - Science des Matériaux
Vol. 50, No. 5, October, 2026, pp. 513-520
Journal homepage: http://iieta.org/journals/acsm

Characterization and Evaluation of Self-Sensing Engineered Cementitious Composites Reinforced with Basalt Fiber

Sara W. N. Al-Shaawi*, Ali M. AL-Dahawi, Hussein H. Zghair

College of Civil Engineering, University of Technology- Iraq, Baghdad 10066, Iraq

Corresponding Author Email: bce.22.36@grad.uotechnology.edu.iq

Copyright: ©2025 The authors. This article is published by IIETA and is licensed under the CC BY 4.0 license (http://creativecommons.org/licenses/by/4.0/).

https://doi.org/10.18280/acsm.500510

Received: 9 May 2026
Revised: 16 July 2026
Accepted: 5 August 2026
Available online: 31 October 2026

Keywords:
basalt fiber, cementitious composites, composite materials, reinforced composite, self-sensing materials, sustainable construction materials

ABSTRACT

The advancement of smart materials in civil engineering has led to the development of self-sensing engineered cementitious composites (ECC), capable of detecting damage in real time. This study explores the mechanical and self-sensing behavior of ECC incorporating basalt fibers engineered cementitious composites (BF-ECC) to improve strain sensitivity, structural strength, and durability. Basalt fibers (BF), derived from volcanic rock, exhibit excellent tensile strength, thermal stability, and corrosion resistance, making them suitable for sensing-enabled cementitious composites. The experimental program evaluated compressive and flexural strengths, electrical resistivity, water absorption, and flowability across ECC mixes with BF content of 0.5%, 1.0%, 1.5%, and 2% by volume. The results showed that 2% BF incorporation led to a 15.6% increase in compressive strength from 30.3 to 35.0 MPa, and a 41.7% increase in flexural strength at 28 days from 6.0 to 8.5 kN. The electrical resistivity improved by 50%, from 3.0 to 4.5 MΩ. Water absorption decreased by 47% to 3.2%, while flowability improved by 5%, reaching 105 mm. These improvements demonstrate that BF-ECC effectively enhances mechanical performance and enables strain-based sensing without compromising workability. The ability to detect early-stage cracking through changes in electrical response supports long-term durability and reduced maintenance in smart infrastructure applications. The study concludes that basalt fiber-reinforced ECC offers a promising, sustainable solution for next-generation construction. Future research should focus on fiber dispersion optimization, hybrid reinforcements, and large-scale implementation strategies to maximize sensing reliability and field applicability.

1. INTRODUCTION

The pursuit of smart and sustainable materials is a growing priority in modern civil construction. Traditional concrete is prone to cracking and deterioration, leading to expensive repairs and structural failures. Engineered cementitious composites (ECC) offer a superior alternative, providing enhanced fracture control, high strength, and excellent flexibility to address these challenges effectively. Li [1] investigated basalt fiber-reinforced ECC with integrated self-sensing capabilities for real-time damage monitoring, aiming to improve mechanical strength, strain-sensing efficiency, and long-term durability.

Designed through micromechanics principles, ECC achieves over 3% strain capacity under load with only 2% fiber by volume, offering high flexibility under both tensile and compressive forces. ECC addresses environmental concerns by offering superior ductility and resilience compared to conventional concrete, effectively preventing crack propagation and lowering maintenance needs. Its tightly controlled crack widths also reduce permeability, enhancing both durability and service life [2].

Sustainable ECC mixtures use supplementary materials like fly ash and fine silica to reduce cement consumption and carbon emissions. Fiber incorporation enhances strength and enables self-sensing functionality. Basalt fibers (BF), in particular, are gaining attention for improving both strength and workability due to their high tensile strength, chemical resistance, and thermal stability, making them an effective reinforcement derived from natural volcanic rock [3, 4].

Recent advancements in construction materials have enabled the development of self-sensing and self-repairing cement composites. These materials can detect structural stress through changes in electrical resistance and autonomously heal minor cracks, thereby enhancing durability and extending service life. Current research strongly focuses on advancing these self-repairing capabilities [5, 6]. Various techniques such as integrating minuscule capsules of therapeutic agents and augmenting natural healing with optimized formulations have been investigated. The objective is to rehabilitate the material's properties following damage, thereby reducing maintenance costs and prolonging its service life [5, 7]. Self-sensing materials can detect strain, stress, and damage through variations in electrical resistance [8].

When subjected to external pressure, ECC combined with conductive materials such as carbon nanotubes, steel fibers, or BF exhibits changes in its electrical conductivity that indicate strain [9]. Basalt fiber enhances the piezoresistive properties

of ECC, enabling real-time structural health monitoring without external sensors. Its incorporation also improves the strength, toughness, and fracture resistance of the composite, making it highly effective for self-sensing applications [10]. Basalt fiber-reinforced ECC outperforms traditional mixes in bending strength, impact resistance, wear durability, and strain-hardening, making it ideal for critical structures such as bridges, tunnels, and seismic zones. In addition to enhancing mechanical performance, BF improves piezoresistive sensitivity, enabling self-sensing functionality.

This study aims to evaluate the self-sensing capabilities of ECC incorporating basalt fiber, with a specific focus on strain-sensing behavior, mechanical strength, and long-term durability. It investigates how basalt fiber affects electrical resistivity, crack propagation, and structural toughness. Experimental methods include resistivity measurement, mechanical testing, and microstructural analysis. The findings will contribute to the development of sustainable, smart cementitious materials that reduce maintenance costs and improve structural safety.

2. MATERIALS AND METHODS

2.1 Materials

Type I ordinary Portland cement (OPC), which is a general-purpose cement suitable for conventional construction applications, was used. The OPC and fly ash properties have been measured, and the measurement results are shown in Tables 1 and 2. The qualities of a local material meet the standards of Iraqi Standard No. (5), 1984 (IQS, 5/1984) [11]. Fly ash type F, with a specific gravity of 2.10, was used as it meets the requirements of the work; pozzolanic characteristics are present in this form of fly ash that complies with [12, 13].

A water tap was used in the process of mixing and treating the concrete samples; silica sand with a diameter of 300 and water absorption capacity (0.30%) was used according to the manufacturer. Figure 1 shows a sample of it with a datasheet. A high-range water-reducing admixture (HRWRA) solution based on polycarboxylate ether was used in all mixtures. Metal electrode placement for self-sensing was used. Samples of the OPC and the fly ash are shown in Figure 1.

Table 1. The characterized physical properties of cement.

Physical Properties of Portland Cement		
Property	**Test Results**	**Limit of IQS 5/1984-Type I [11]**
Specific surface area by the Blaine method (m^2/kg)	367	≥230
Setting time		
-Initial	02:04	≥45 min
-Final	04:00	≤10 h
Compressive strength (MPa)		
3 days	20	≥15
7 days	29.5	≥23
Soundness (autoclave) %	0.05	≤0.8
Physical properties of fly ash		
Specific gravity		2.10
Blaine fineness (cm^2/g)	2690	

Note: Iraqi Standard No. (5), 1984 (IQS, 5/1984) [11].

Basalt fiber properties have been measured according to the American Society for Testing and Materials (ASTM) International 2022 [14]. The characterization results are shown in Table 3. The basalt fiber, shown in Figure 2, was used to enhance the mechanical properties and make the arrays electrically conductive for the self-sensing test and the ability to know the changes in electrical resistance during the application of different loads [15]. These fibers were used with a length of 13 mm, filament diameter of 16 µm, moisture ≥ 0.2, tensile strength of 3,550 MPa, and elastic modulus ≥ 40 GPa. Table 3 shows the properties of basalt fiber.

Table 2. Chemical composition of Portland cement and fly ash

Chemical Composition	Portland Cement (wt.%)	IQS 5/1984	Fly Ash (wt.%)
CaO	66.11	No limit	7.98
SiO_2	21.93	No limit	52.22
Al_2O_3	4.98	No limit	16.58
Fe_2O_3	3.1	No limit	6.60
MgO	2	6.0% max	2.10
SO_3	2.25	3.5% max	0.02
Loss on ignition (LOI)	2.39	3.0% max	10.36
C_3S	58.52	No limit	—
C_2S	19	No limit	—
C_3A	7.95	No limit	—
C_4AF	9.43	No limit	—

Note: Iraqi Standard No. (5), 1984 (IQS, 5/1984) [11].

Table 3. Properties of basalt fiber

Item	Unit	Standard Value
Line density	Tex	±8
Filament diameter	µm	16
Moisture	%	≤0.2
Tensile strength	MPa	≥3,550
Elastic modulus	GPa	≥40
Break strength	N/tex	≥0.4
Tensile rate of break	%	≤3.0
Appearance	No stains, impurities, hairiness, or other defects; uniform color, dark brown, rich in metallic luster.	



Figure 1. Portland cement and fly ash



Figure 2. Basalt fiber used as reinforcement agent

2.2 Methods of mixture design, casting, and curing

The dry materials were mixed first with basalt fiber, and water containing superplasticizer was added gradually. This method was the most suitable for completing this work under laboratory conditions, as the consistency of the basalt has a great effect on the workability of the mixture. In this way, a suitable consistency was obtained with good flow. After that, the molds were prepared according to the specifications; the molds were greased before the casting process, and the mixture was poured and left for approximately 24 hours. After that, the molds were opened for the purpose of treatment and examination. The BF were cured in three ways to meet the research requirements. The observed is depicted in Figure 3. Some of the samples were cured in water and examined at various stages of age. Part of the samples were cured with air, where they were immersed in water for a week to complete the hydration process. After that, they were examined at various stages of age, and part of the samples were cured directly with a carbonation device and examined at various stages of age [16]. Additional details can be found in Table 4.



Figure 3. Mixing and casting of the test samples

Table 4. The quantities of materials used in the mixture

No.	Mixture Designation	Cement (g)	Sand (g)	Fly Ash (g)	W/C	Fiber (g)
1	The reference mix	566	453	680	0.27	0
2	0.5% basalt fiber	566	453	680	0.27	13.5
3	1% basalt fiber	566	453	680	0.27	26
4	1.5% basalt fiber	566	453	680	0.27	40.5
5	2% basalt fiber	566	453	680	0.27	54

Note: Water-to-cement ratio (W/C).

2.3 Testing methodologies

Tests were conducted on fresh and dry samples to determine the effect of fiber on the mechanical properties of the mixture. In the fresh state, flow tests were conducted, and in the dry state, compression, flexural, permeability, density, absorption, electrical conductivity, and crack width tests were conducted.

2.3.1 Flow test

The flow is the resulting increase in average base diameter of the mortar mass, expressed as a percentage of the original base diameter. The flow testing table, shown in Figure 4, was carefully wiped, cleaned, and dried, and then the flow mold was placed in the middle of the table. A layer of mortar about 25 mm thick was placed in the mold and pressed 20 times with the tamping rod. Then a second layer was placed and compacted with the tamping rod, also 20 times. Once finished, the mold was lifted, and 25 strokes were made with the device within 15 seconds, followed by three diameter readings with a vernier, and the average was considered [17].



Figure 4. Flow test apparatus

2.3.2 Compressive strength test

The compressive strength testing machine, shown in Figure 5, was used to test cube samples of size (50 × 50 × 50) mm. According to the test machine, an ELE hydraulic compression system with a 2,000 kN capacity was used, with a rate of 0.3 N/mm²/s [18]. The average strength was calculated from three samples per mixture, and the tests were performed at 7 and 28 days of curing [19]. This process is further explained in Figure 5.



Figure 5. Compressive strength testing machine

2.3.3 Flexural strength test

ECC exhibits superior tensile properties due to its unique microstructure and fiber reinforcement, which help control cracking and enhance load-bearing capacity [20]. The flexural strength test was performed on samples measuring 40 × 40 × 160 mm using the cement mortar testing device. The samples were tested at 7 and 28 days of age using the Flexural Strength Test machine shown in Figure 6.



Figure 6. Flexural strength test

2.3.4 Dry density test

The density of concrete is determined after removing the cubes from the curing water and drying the surfaces with a cloth. The density is calculated from the mass of the sample obtained after drying, and its volume is 50 × 50 × 50, as per ASTM International 2021 [21].

2.3.5 Absorption test

The test is carried out according to the specification, with the absorption test performed after immersion in water, and the cube samples are dried in an oven at 100–110 ℃ for at least 24 hours. After removing the samples from the oven, they are dried in dry air at a room temperature of 20–25 ℃. This is further shown in Figure 7. Then the mass is calculated; the sample is immersed in water for 48 hours, then removed, and the surface is dried with a wet cloth, and the mass is recalculated according to this study [21].



Figure 7. Absorption test

2.3.6 Compressive testing and electrical resistivity measurement

In this test, samples cast in molds of size (50 mm) were used, and the test was conducted according to the specification of ASTM International 2022 [14]. The compression test was conducted on three samples of each ratio and analyzed throughout the test. ELE test machine with a capacity of 2,000 kN and a loading rate of 0.9 kN/sec was used to perform the test and was subjected to continuous loading until failure occurred .

During the compression test, the direct current (DC) electrical resistance along the loading direction was measured using binary probes installed in two symmetrical planes. The probes were positioned at mid-height of the specimen and oriented perpendicular to the stress axis to ensure consistent and reliable measurements. DC measurements were performed according to the approach proposed by Wen and Chung [22] and recorded with a Pro'sKit MT-1860 digital multimeter. To prevent any unintended electrical interference during loading, a non-conductive wooden or plastic barrier was placed between the loading platens and the specimen. The measured electrical conductivity data were subsequently processed and converted into the fractional change in electrical resistivity, as described by Al-Dahawi [23], allowing evaluation of the electrical response of the specimens under compressive loading. This process is further explained in Figure 8.

This study involves two electrode strips made from a brass plate, each 0.1 mm thick, with a resistance of 0.3 Ω, a length of 7.5 cm (5 cm within the cube and 2.5 cm external), and a width of 1 cm. These strips were symmetrically positioned around the midpoint of the sample, with 40 mm separation following the procedure reported by Ahmed et al. [24].



Figure 8. Electrical resistivity measurement under different loads

3. RESULTS AND DISCUSSION

3.1 Results and analysis of flowability test

The flowability (slump) of ECC increased with higher basalt fiber content, rising from 90 mm at 0.5% fiber dosage to 104 mm at 2%. In contrast to other fiber types, which typically reduce workability by increasing internal friction within the matrix, BF appear to enhance flowability at higher dosages. This improvement may be attributed to a fiber-lubrication effect, wherein the BF reduce inter-particle friction, facilitating smoother flow. The lowest flowability was observed at 0.5% fiber content (90 mm), indicating a stiffer mix that might require the use of additional water-reducing admixtures to achieve the desired workability. Conversely, the mix containing 2% basalt fiber exhibited the highest flowability of 104 mm, demonstrating that ECC remains highly workable and self-consolidating even at elevated fiber volumes. A flow value exceeding 100 mm can be advantageous for placing ECC into complex formwork without the need for extensive vibration or compaction. However, it is important to note that excessive flowability may lead to segregation, potentially causing uneven fiber distribution, which could adversely affect the composite's mechanical performance. Flowability trends with different fiber dosages are depicted in Figure 9.

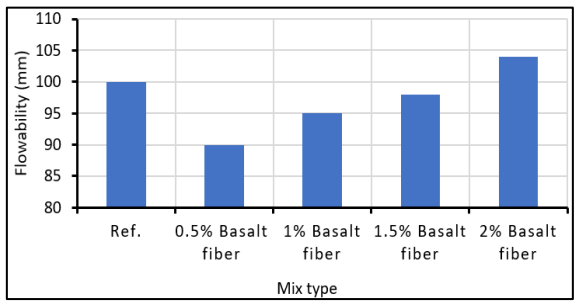


Figure 9. Flowability (slump) of engineered cementitious composites (ECC) as a function of basalt fiber content

3.2 Compressive strength test

The reference mix demonstrated a 7-day compressive strength of 24.4 kN. The incorporation of 0.5% basalt fiber increased the early-age strength to 26.2 kN, resulting in a 7.4% improvement. However, as the proportion of basalt fiber exceeded 0.5%, there was no significant increase in weak strength. The values for 1%, 1.5%, and 2% fiber content ranged from 25.7 kN to 26.0 kN, indicating little variation.

The results indicate that 0.5% basalt fiber enhances initial water absorption and enhances the mixture's support; nevertheless, an increased fiber content does not significantly improve early strength. This may result from fiber aggregation or weak bonding during the initial setup phase.

After 28 days, the reference mix had a 28-day squash strength of 32.5 kN. With 0.5% basalt fiber, the strength increased to 35.4 kN, exhibiting a significant 8.9% improvement over the control blend. Similar to the 7-day results, increasing the fiber concentration above 0.5% did not yield significant strength improvements, with measurements from 34.4 kN to 35.1 kN for 1%, 1.5%, and 2% fiber content. The little reduction in push strength at higher fiber concentrations (1% and above) may result from the disintegration of the fiber matrix or uneven distribution of fibers, leading to vulnerabilities in the mixture.

The maximum compressive strength of 26.2 and 35.4 kN at 7 days and 28 days, respectively, was observed with 0.5% basalt fiber. Beyond this juncture, the compressive strength diminishes slightly, suggesting that an excess of basalt material may introduce additional vulnerabilities due to fiber aggregation and potential voids. This indicates that 0.5% rock fiber is the optimal quantity for enhancing compressive strength in this ECC mixture. The reference mix exhibited a 33.2% increase in strength from 7 to 28 days (24.4 kN to 32.5 kN).

The 0.5% basalt fiber blend exhibited a 35.1% increase in strength (26.2 kN to 35.4 kN), indicating that fiber reinforcement contributed to enhanced durability and strength development during prolonged moisture exposure. The 1%, 1.5%, and 2% fiber mixtures exhibited a more consistent growth range of approximately 34%, indicating that the self-supporting properties of basalt fiber help maintain strength over time. The evolution of compressive strength at early and late stages is summarized in Figure 10.

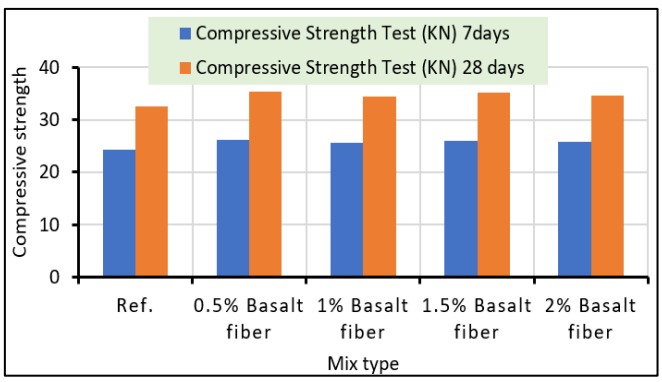


Figure 10. Variation in compressive strength of engineered cementitious composites (ECC) mixtures with different basalt fiber contents

3.3 Flexural strength test

The evolution of flexural strength at different testing ages is presented in Figure 11. At an early testing age of 7 days, the reference ECC mix exhibited the lowest flexural strength of 2.7 kN, indicating the limited bending resistance of plain ECC without fiber reinforcement. The incorporation of basalt fiber significantly enhanced flexural performance at this age. The highest flexural strength was recorded for the mix containing 1.5% basalt fiber, reaching 4.98 kN, which represents an 84% increase compared with the reference mix. This improvement confirms the effectiveness of BF at an early age, where fiber bridging across microcracks enhances tensile resistance and post-cracking load-carrying capacity. The superior performance of the 1.5% fiber mix at an early age suggests that this fiber dosage is particularly beneficial for short-term flexural performance.

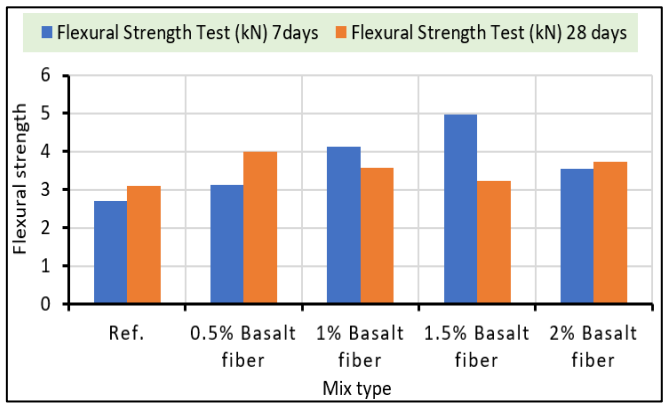


Figure 11. Flexural load-deflection curves for different fiber dosages

At a later testing age of 28 days, a different trend was observed. The maximum flexural strength was achieved by the mix containing 0.5% basalt fiber, which reached 4.0 kN, corresponding to a 29% enhancement relative to the reference mix. In contrast, mixes with fiber contents of 1%, 1.5%, and 2% exhibited reductions in flexural strength relative to their early-age values. In particular, the 1.5% fiber mix showed a notable decrease in strength at the later age, reaching 3.24 kN.

The mix incorporating 2% basalt fiber demonstrated variable behavior, achieving a flexural strength of 3.72 kN at a later age. Although this value exceeded that of the 1.5% mix, it remained lower than the strength recorded for the 0.5% fiber mix. These findings indicate that excessive fiber content may adversely influence flexural strength development at later ages. Among all mixtures, the ECC containing 0.5% basalt fiber exhibited the most stable strength development with age, achieving the highest later-age flexural strength while maintaining adequate workability and effective fiber–matrix interaction.

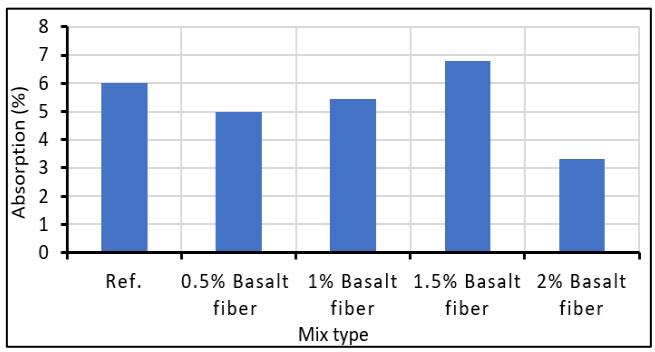


Figure 12. Water absorption vs. basalt fiber dosage in

engineered cementitious composites (ECC) specimens

3.4 Absorption test

The reference mix exhibited the highest water absorption, at 6%, indicating increased porosity and a probable susceptibility to moisture. At a basalt fiber content of 0.5%, absorption decreased to 5%, indicating enhanced fiber-matrix interaction, which reduces microcracks and voids within the composite. Figure 12 illustrates the effect of basalt fiber on water absorption, showing nonlinear behavior. At 1% fiber content, absorption rose little, by 5.45%, presumably due to the elevated fiber volume influencing mix density. With a fiber content of 1.5%, absorption rose to 6.8%, surpassing the reference mix, indicating that at this concentration, fiber aggregation or excessive porosity may adversely affect impermeability. The lowest absorption of 3.3% was seen at 2% fiber content, suggesting enhanced densification and matrix filling, maybe resulting in a more impermeable composite.

3.5 Dry density test

The reference mix had the lowest dry density of 2,000 kg/m³, serving as the baseline ECC mix. The 0.5% fiber inclusion increased the density to 2,152 kg/m³, signifying enhanced packing efficiency and matrix reinforcement. The 1% fiber content further increased density to 2,200 kg/m³, continuing the trend of improved compactness. The 1.5% fiber content resulted in an increase to 2,320 kg/m³, suggesting that at this level, fibers effectively fill voids and strengthen the cementitious matrix. 2% fiber content yielded the highest density of 2,400 kg/m³, confirming that higher fiber dosages result in a denser, more compact material. The dry density results presented in Figure 13 indicate a steady increase with higher fiber dosage.

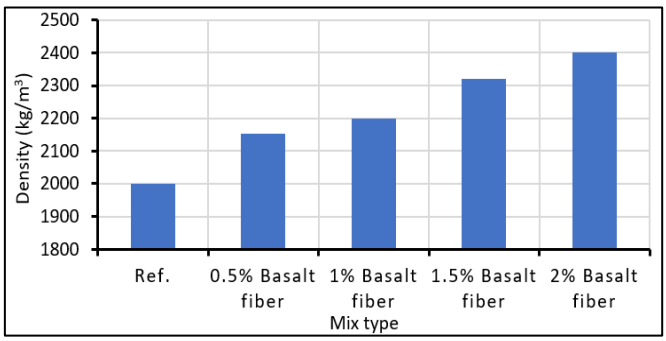


Figure 13. Variation of dry density with basalt fiber content in engineered cementitious composites (ECC)

3.6 Compressive testing and electrical resistivity measurement

The increase in compressive strength at 0.5% fiber content is attributed to the reinforcing properties of BF, which facilitate bridging of microcracks and improve load distribution. The findings are similar to the results of Han et al. [25]. Elevated fiber concentrations of 1.5% to 2% may result in fiber clustering or poor dispersion, causing voids that slightly reduce strength (2). The variations in strength between 1% and 2% fiber content indicate an appropriate fiber volume fraction (~0.5%–1.5%) beyond which fibers do not substantially enhance compressive strength [26]. The consistent rise in electrical resistance with fiber content indicates that BF enhance the self-sensing capability of ECC [27]. Higher fiber concentrations provide additional discontinuities within the cementitious matrix, enhancing resistivity and enabling their utilization for structural health monitoring applications. As shown in Figure 14, both compressive strength and electrical resistance are affected by the basalt fiber content. This tendency aligns with a previous study [28] which demonstrated that fiber-matrix interactions influence conductivity, with higher fiber volumes enhancing piezoresistive response.

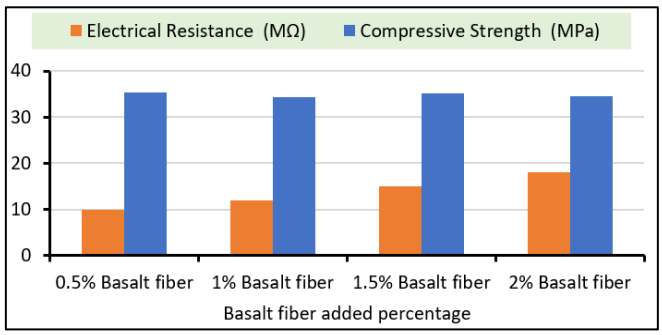


Figure 14. Correlation between compressive strength and electrical resistivity of engineered cementitious composites (ECC) with various percentages of basalt fiber additive

4. CONCLUSIONS

This study focused on evaluating the mechanical and self-sensing performance of ECC reinforced with varying basalt fiber. The main objective was to investigate how basalt fiber influences the strength, crack resistance, and piezoresistive response of ECC, thereby determining its potential as a cost-effective and durable alternative to traditional carbon-based smart composites. Based on the experimental results, the following conclusions can be drawn:

•Mechanical Flexural strength increased significantly with basalt fiber, providing superior crack resistance and improved ductility. Compressive strength showed a moderate improvement, confirming that fibers primarily enhance tensile rather than compressive strength. However, excessive fiber content reduced workability and increased fiber clustering, which negatively affected performance.

•On the Self-Sensing Performance, the incorporation of basalt fiber improved the piezoresistive response of ECC, allowing detection of strain and damage through measurable changes in electrical resistivity. A stable and repeatable self-sensing behavior was observed at 1.0–1.5% fiber content.

•Durability, characterized by water absorption, decreased at lower basalt fiber contents, improving impermeability and resistance to moisture ingress. The optimal basalt fiber content for balancing self-sensing performance, mechanical properties, and constructability was found to be 0.5–1.5% by volume.

AUTHOR CONTRIBUTIONS

Conceptualization, Sara Nasser, Ali AL-Dahawi; methodology, Sara Nasser, Ali AL-Dahawi, Hussein Zghair; software, Sara Nasser; validation, Sara Nasser, Ali AL-Dahawi, Hussein Zghair; formal analysis, Sara Nasser, Ali AL-Dahawi, Hussein Zghair; investigation, Sara Nasser;

resources, Ali AL-Dahawi, Hussein Zghair; data curation, Sara Nasser, Ali AL-Dahawi, Hussein Zghair; writing-original draft preparation, Sara Nasser; writing-review and editing, Ali AL-Dahawi, Hussein Zghair; supervision, Ali AL-Dahawi, Hussein Zghair. All authors have read and agreed to the published version of the manuscript.

FUNDING

This work has not received any financial funding. However, measurements and testing equipment were made available by the College of Civil Engineering at the University of Technology, Iraq.

REFERENCES

[1] Li, V.C. (2003). On engineered cementitious composites (ECC) a review of the material and its applications. Journal of Advanced Concrete Technology, 1(3): 215-230. https://doi.org/10.3151/jact.1.215

[2] Li, V.C., Kanda, T. (1998). Innovations forum: Engineered cementitious composites for structural applications. Journal of Materials in Civil Engineering, 10(2): 66-69. https://doi.org/10.1061/(ASCE)0899-1561(1998)10:2(66)

[3] Hosny, O.M., Yasien, A.M., Bassuoni, M.T., Gourlay, K., Ghazy, A. (2024). Cementitious composites with cellulose nanomaterials and basalt fiber pellets: Experimental and statistical modeling. Fibers, 12(1): 12. https://doi.org/10.3390/fib12010012

[4] Borra, R., Meesaraganda, L.V.P. (2026). Basalt fiber–reinforced self-compacting concrete: A functionally graded approach for enhanced flexural resistance. Journal of Structural Design and Construction Practice, 31(1): 04025137. https://doi.org/10.1061/JSDCCC.SCENG-1842

[5] Al-Dahawi, A.M., Abdullah, R.D., Joni, H.H. (2024). An investigation of self-sensing and mechanical properties of smart engineered cementitious composites reinforced with functional materials. Open Engineering, 14(1): 20220568. https://doi.org/10.1515/eng-2022-0568

[6] Bekzhanova, Z., Memon, S.A., Kim, J.R. (2021). Self-sensing cementitious composites: Review and perspective. Nanomaterials, 11(9): 2355. https://doi.org/10.3390/nano11092355

[7] Siad, H., Lachemi, M., Sahmaran, M., Hossain, A. (2017). Multi-functional cementitious composites with sensing and healing capabilities. Proceedings of International Structural Engineering and Construction, 4(1): 1-6.

[8] Han, B., Ding, S., Yu, X. (2015). Intrinsic self-sensing concrete and structures: A review. Measurement, 59: 110-128. https://doi.org/10.1016/j.measurement.2014.09.048

[9] D'Alessandro, A., Rallini, M., Ubertini, F., Materazzi, A.L., Kenny, J.M. (2016). Investigations on scalable fabrication procedures for self-sensing carbon nanotube cement-matrix composites for SHM applications. Cement and Concrete Composites, 65: 200-213. https://doi.org/10.1016/j.cemconcomp.2015.11.001

[10] Kim, M.K., Kim, D.J., An, Y.K. (2018). Electro-mechanical self-sensing response of ultra-high-performance fiber-reinforced concrete in tension. Composites Part B: Engineering, 134: 254-264. https://doi.org/10.1016/j.compositesb.2017.09.061

[11] Al-Jiboory, Y.M., Al-hazaa, S.H. (2022). Assessment of altawseea ordinary Portland cement northern Iraq: Mineralogy, microstructure, and hydration. The Iraqi Geological Journal, 55(2C): 200-210. https://doi.org/10.46717/igj.55.2C.15ms-2022-08-28

[12] ASTM International. (2014). ASTM C618-14: Standard specification for coal fly ash and raw or calcined natural pozzolan for use in concrete. ASTM International, West Conshohocken, PA, USA. https://doi.org/10.14359/51725994

[13] Alhifadhi, M., Al-Attar, T., Hasan, Q. (2023). A proposed new mix proportioning method for fly ash-based geopolymer concrete. Engineering and Technology Journal, 41(11): 1346-1354. https://doi.org/10.30684/etj.2023.139354.1427

[14] ASTM International. (2022). ASTM D8448/D8448M-22: Standard specification for basalt fiber strands. ASTM International, West Conshohocken, PA, USA. https://doi.org/10.1520/D8448_D8448M-22

[15] Tavadi, A.R., Naik, Y., Kumaresan, K., Jamadar, N.I., Rajaravi, C. (2021). Basalt fiber and its composite manufacturing and applications: An overview. International Journal of Engineering, Science and Technology, 13(4): 50-56. http://doi.org/10.4314/ijest.v13i4.6

[16] ASTM International. (2002). ASTM C192/C192M–02: Standard practice for making and curing concrete test specimens in the laboratory. ASTM International, West Conshohocken, PA, USA. https://doi.org/10.1520/C0192_C0192M-02

[17] ASTM International. (2015). ASTM C1437–15: Standard test method for flow of hydraulic cement mortar. ASTM International, West Conshohocken, PA, USA. https://doi.org/10.1520/C1437-15

[18] Al-Masraf, H., Al-Attar, T., Freyyah, Q. (2024). Mechanical and thermal performance of engineered cementitious composite concrete produced by using polyvinyl alcohol fibers. Engineering and Technology Journal, 42(11): 1290-1303. https://doi.org/10.30684/etj.2024.146641.1691

[19] ASTM International. (2002). ASTM C109/C109M–02: Standard test method for compressive strength of hydraulic cement mortars. ASTM International, West Conshohocken, PA, USA. https://doi.org/10.1520/C0109_C0109M-02

[20] ASTM International. (2008). ASTM C348-08: Standard test method for flexural strength of hydraulic-cement mortars. ASTM International, West Conshohocken, PA, USA. https://doi.org/10.1520/C0348-08

[21] ASTM International. (2021). ASTM C642-21: Standard test method for density, absorption, and voids in hardened concrete. ASTM International, West Conshohocken, PA, USA. https://doi.org/10.1520/C0642-21

[22] Wen, S., Chung, D.D.L. (1999). Piezoresistivity in continuous carbon fiber cement-matrix composite. Cement and Concrete Research, 29(3): 445-449. https://doi.org/10.1016/S0008-8846(98)00211-7

[23] Al-Dahawi, A. (2016). Multifunctional cementitious composites for damage-resistant highway structures. University of Gaziantep, Gaziantep, Turkey.

[24] Ahmed, S., Al-Dahawi, A., Hassan, S. (2025). Self-sensing engineered cementitious composites with carbon nanotubes and reinforcing fibers for damage detection. Engineering and Technology Journal, 43(11): 852-865. https://doi.org/10.30684/etj.2025.156508.1879

[25] Han, B., Sun, S., Ding, S., Zhang, L., Yu, X., Ou, J. (2015). Review of nanocarbon-engineered multifunctional cementitious composites. Composites Part A: Applied Science and Manufacturing, 70: 69-81. https://doi.org/10.1016/j.compositesa.2014.12.002

[26] Wang, Y., Wang, Y., Wan, B., Han, B., Cai, G., Chang, R. (2018). Strain and damage self-sensing of basalt fiber reinforced polymer laminates fabricated with carbon nanofibers/epoxy composites under tension. Composites Part A: Applied Science and Manufacturing, 113: 40-52. https://doi.org/10.1016/j.compositesa.2018.07.017

[27] Al-Dahawi, A., Sarwary, M.H., Öztürk, O., et al. (2016). Electrical percolation threshold of cementitious composites possessing self-sensing functionality incorporating different carbon-based materials. Smart Materials and Structures, 25(10): 105005. https://doi.org/10.1088/0964-1726/25/10/105005

[28] Wang, Z.B., Han, S., Sun, P., Liu, W.K., Wang, Q. (2021). Mechanical properties of polyvinyl alcohol-basalt hybrid fiber engineered cementitious composites with impact of elevated temperatures. Journal of Central South University, 28(5): 1459-1475. https://doi.org/10.1007/s11771-021-4710-1